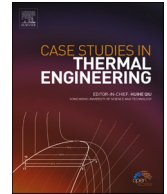




ELSEVIER

Contents lists available at ScienceDirect

Case Studies in Thermal Engineering

journal homepage: www.elsevier.com/locate/csite

Improving the thermal characteristics of a cooling tower by replacing the operating fluid with functionalized and non-functionalized aqueous MWCNT nanofluids

Nazanin Karimi Bakhtiyar^a, Reza Javadpour^a, Saeed Zeinali Heris^{a,*},
Mousa Mohammadpourfard^{a,b}

^a Faculty of Chemical and Petroleum Engineering, University of Tabriz, Tabriz, Iran

^b Department of Energy Systems Engineering, Izmir Institute of Technology, Izmir, Turkey

ARTICLE INFO

Keywords:

MWCNTs

Water loss

Cooling tower thermal performance

Zeta potential

DLS

Functionalized carbon nanotubes nanofluids

ABSTRACT

In this study, the thermal properties of the operating fluid by replacing the fluid with better thermal properties and lower water loss in a cross-flow cooling tower (CFWCT) investigated. For this purpose, MWCNTs/H₂O, MWCNTs-COOH/H₂O, and MWCNTs-OH/H₂O nanofluids were used instead of water, and the results were compared. The visual method and dynamic light scattering (DLS) were used to guarantee the stability of nanofluids and to determine the size distribution of the nanoparticles in the nanofluid. The influence of nanofluids concentration on cooling towers performance variables such as evaporation rate, performance characteristics, temperature drop, and tower efficiency were investigated. The results showed that the functionalized nanofluids with lower evaporation rates than water and the non-functionalized nanofluids with higher evaporation rates than water improved the thermal performance of CFWCT. For example, at a concentration of 0.1 wt% MWCNTs-COOH/H₂O, MWCNTs-OH/H₂O, and MWCNTs/H₂O, the efficiency of the cooling tower was 46%, 45.3%, and 43.2%, and the performance characteristics were improved by 15.8%, 11.2%, and 6.1%, respectively, compared with water. Among the nanofluids, MWCNTs-COOH/H₂O nanofluid had the best performance, in which the evaporation rate, performance characteristics, temperature drop, and efficiency were increased by about -4.3%, 15.8%, 15.9%, and 8.7%, respectively, compared to water.

Nomenclature

a_{fi}	Interfacial surface area between air and water per unit volume of fill zone(m^{-1})
A_{fi}	Frontal area of fill perpendicular to air flow direction(m^2)
C	Evaporative capacity rate ratio ($kg s^{-1}$)
C_p	Specific heat at constant pressure ($J kg^{-1}K^{-1}$)
CFWCT	Cross flow wet cooling tower
G	Mass velocity ($kg m^{-2} s^{-1}$)
h_d	Mass transfer coefficient ($m s^{-1}$)

* Corresponding author.

E-mail address: s.zeinali@tabrizu.ac.ir (S. Zeinali Heris).

<https://doi.org/10.1016/j.csite.2022.102422>

Received 15 June 2022; Received in revised form 18 August 2022; Accepted 8 September 2022

Available online 9 September 2022

2214-157X/© 2022 The Author(s).

Published by Elsevier Ltd.

This is an open access article under the CC BY license

(<http://creativecommons.org/licenses/by/4.0/>).

I	Specific enthalpy (J kg^{-1})
K	Air flow rate (kg s^{-1})
m	Mass flow rate (kg s^{-1})
M	Calculated quantity from the measurable parameter
Me	Merkel number
NTU	Number of transfer units
L_{fi}	Fill length (m)
Q	Heat (W)
T	Temperature ($^{\circ}\text{C}$)
T_R	Cooling range ($^{\circ}\text{C}$)
U	Maximum error
wt	Particle weight fraction (%)
y	Measurable parameters
X	Specific humidity of the air

Greek symbols

ϵ	Effectiveness of the cooling tower
λ	Correction factor (pure number)

Subscripts

a	Air
bf	Base fluid
i	Inlet
ma	Air-vapor (per kg dry air)
min	Minimum
max	Maximum
p	Particle
o	Outlet
s	Saturated
w	Water

1. Introduction

Cooling towers and other evaporative heat removal systems have traditionally been used in various applications, including power generation, refrigeration cycles, and industrial processes that require the removal of large amounts of waste heat. Evaporative cooling systems, such as cooling towers, operate on the principle of direct contact between water and unsaturated air. Mass transfer occurs in terms of the vapor pressure difference between the gaseous and liquid phases. The more water evaporates and cools, the more the air is humidified and heated [1,2]. Cooling towers have three categories of flow patterns: parallel flow, cross flow, and counter flow. The water spray, fill, and rain zones are all heat and mass transfer zones in wet cooling towers. In terms of using a fan, cooling systems are divided into natural draft and mechanical draft cooling towers [3,4].

Extensive research was conducted in the last decade to increase the efficiency of cooling towers. Most classical research on cooling towers falls into several categories. A number of studies examined the effects of process factors such as water and air flow rates and water inlet temperature in cooling towers. All of them concluded that as the air flow rate increases and the circulating water flow rate decreases, and the water inlet temperature increases, the cooling process of the tower increases, thus improving its performance. Other studies addressed the impact of environmental factors including temperature, humidity, and ambient wind speed, as well as the geometric shape and physical components of cooling towers, and several studies on the prediction of cooling tower performance under various conditions [5,6].

Lyu et al. [7] used a 3-D numerical model to investigate the effect of different packing arrangements on cooling tower performance. They found that the non-uniform arrangement can improve the performance of the cooling tower in both crosswind and windless states. Dmitriev et al. [8] created a novel inclined corrugated fill bed for use in an experimental cooling tower, complete with perforations and an inclined plate to ensure uniform distribution of the air-water contact zone. The effect of fill bed design on cooling tower thermal performance was studied, and four empirical correlations for pressure drop in dry fill beds were obtained. They concluded that the tower performs best with low humidification rates and that inclined plates with a perforation diameter of 6 mm provide the best mass and heat transfer performance as well as the lowest pressure drop. Ayoub et al. [9] evaluated the influence of external environmental factors on the wet cooling tower performance. Their results indicated that even a small increase in temperature above the design temperature of the cooling tower significantly impacts its efficiency. The ϵ -NTU method was used by Pandelidis [10] to perform a numerical study of the Maisotsenko cycle (M-cycle) cooling tower. The numerical study explored the most important factors for cooling tower efficiency and found that an M-cycle cooling tower can reduce the water temperature below the wet-bulb temperature of the air inlet. Jianhang et al. [11] studied a counter flow cooling tower including a coupling model in which the

performance of the cooling tower was based on packing analysis and the rain and spray zones. The results showed that by reducing the diameter of water droplets and increasing the ambient humidity, the efficiency of the cooling tower increased. Wang et al. [12] found that using an enclosure with an opening on the windward side increased the performance of the cooling tower in crosswind conditions.

Few studies were conducted on replacing the working fluid of cooling towers with a fluid that has better thermal properties than ordinary water. Using such a working fluid improves the efficiency of the cooling tower. Many researchers have recently developed an interest in the colloidal suspension of nanoparticles in base fluids called nanofluids, which are employed as working fluids in various fields [13,14]. Nano-additives are used in various industrial fields, e.g. to optimize the efficiency of thermal systems, mass and heat transfer [15], or in the environmental field, e.g. as adsorbents [16] in water treatment and CO₂ capture [17] for zero emissions. Nanofluids have been created using a range of nano additions, including metals and metal oxides [18,19] and carbon-based nanomaterials [20]. It was shown that the addition of nanoparticles to base fluids can significantly improve their thermal properties while reducing the pressure drop and sedimentation problems that are common with larger particles. However, the biggest challenge to using nanofluids in the industry is the stability of nanoparticles in base fluids. Researchers have used various methods in recent years to improve the stability of nanoparticles in base fluids. One of these methods involves using surfactants. Therefore, selecting the right surfactant and nanoparticle for each application is critical [21,22].

The following studies investigated the performance of a cooling tower using nanofluid as the working fluid. Imani Mofrad et al. [23] surveyed the effects of six different types of filled beds on cooling tower performance using nanofluid with ZnO nanoparticles as the operating fluid. They observed that the metal mesh bed performs the best. In another study, Imani Mofrad et al. [24] evaluate the effects of various nanoparticles on cooling tower performance, including graphene, ZnO, Al₂O₃, and SiO₂. According to their results, the nanofluid containing graphene nanoparticles improves the cooling tower performance the most. Thus, the addition of 0.02 wt% graphene nanoparticles to the base fluid improves the cooling tower characteristic, volumetric heat transfer coefficient, and efficiency by 36%, 36.2%, and 8.3%, respectively. Elsaid [25] used magnesium oxide and titanium dioxide nanofluids for a feasibility study of a cooling tower with an air conditioning system. In this experimental study, various parameters such as the spacing of the filling blades, the type of filling, and the weight fraction of the nanofluid were investigated. The cooling tower with magnesium oxide nanofluid performed better than the cooling tower with titanium dioxide nanofluid, according to the results. Using copper oxide and aluminum oxide nanofluids, Amini et al. [26] studied the effects of parameters such as type and concentration of nanofluids, the mass flow ratio of working fluid to air, and inlet temperature of nanofluid on the performance of cooling towers. They found that the use of nanofluid improves the performance of cooling towers and that this improvement depends on the type, concentration, and inlet temperature of the nanofluid. Javadpour et al. [27] assessed the effects of packed beds for cross-flow cooling towers and concluded that the use of splash-type packed beds is more relevant when the working fluid is a nanofluid. In another investigation, Javadpour et al. [28] studied the effects of operating parameters on the performance of a cross-flow cooling tower using MWCNTs-water nanofluid as the working fluid. Their first result was the selection of gum arabic among three surfactants as the most suitable surfactant for use in the cooling tower. The nanofluids had a greater impact on cooling tower performance at lower flow rates, their research showed. They optimized operating conditions, including nanofluid concentration and flow rate, to reduce energy consumption and process costs. Rahmati [29] conducted an experiment to determine the effect of ZnO nanofluid on the thermal performance of a wet cooling tower at various concentrations and packing types. It was observed that adding ZnO nanoparticles to the water improves cooling efficiency.

Carbon materials such as graphene, MWCCNT, and diamond play a vital role in boosting the efficiency of heat transfer systems. However, transferring the excellent intrinsic properties of carbon nanoparticles into real-world applications of the corresponding heat transfer fluids remains a challenge [30–32]. Among all other forms of nanoscale materials, carbon-based nanomaterials have the highest thermal conductivity in the literature [33]. The widespread use of these nanoparticles is seen in various fields to increase the performance of solar collectors or to increase the cooling capacity of refrigerators [34,35]. Józwiak et al. [36] investigated numerous effects of carbon-based nanoparticles (MWCNTs, SWCNTs) on thermal conductivity. The results show that the thermal conductivity could be improved by 43.9% and 67.8% for 1 wt% MWCNTs and SWCNTs nanoparticles, respectively. Another study examined the effects of graphene nanoplatelets as well as multi-walled carbon nanotubes to improve diesel oil performance. The result was an improvement in thermal conductivity and electrical conductivity of both nanofluids compared to the pure diesel oil [37]. Matsubara et al. [38] conducted that, by molecular dynamics simulation, the thermal conductivity of a single nanodiamond with 2.5 nm in diameter. the results showed that a nanodiamond with a larger diamond core tends to have a higher thermal conductivity.

MWCNT nanofluids have shown significant improvement in thermophysical parameters such as thermal conductivity when evaluating the heat transfer properties of cooling systems and are about 5 times more useful than other conventional materials [39]. Thus, the development of heat transfer rate is influenced by the higher thermal properties of MWCNTs nanofluids [40]. The major problems with carbon nanotubes for use in various applications are insufficient dispersibility and stability in various organic and aqueous solvents. The second problem of carbon nanostructures is their poor interaction with other materials. Functionalization, a popular method proposed by many researchers, can be used to improve this property [41,42]. Although nanofluids containing MWCNTs have high conductivity, their functionalization significantly increases their conductivity and stability compared to conventional nanofluids [43,44]. The application of MWCNTs in refrigeration systems is new. For instance, in a study that used R600a in MWCNT nano lubricant as a substitute for R134a refrigerant, the performance of household refrigerator systems was examined. Better cooling performance and lower power usage were the outcomes, due to the significant impact of MWCNTs nanoparticles, which were examined in another study [45]. The power consumption of the refrigerator compressor with MWCNT and TiO₂ nano lubricants lowers within the range of 0.9–25.5% and 6.1–18.0%, respectively [46].

Classical research on cooling towers has addressed the process, environment, size, physical components of the tower, and numerical research, as indicated by previous research. Moreover, the most important research on cooling towers was conducted on counterflow cooling towers. The reason may be the complexity and difference in the calculation of cross-flow cooling towers in terms of the

temperature gradient in horizontal and vertical directions. In the majority of studies, heat transfer of water as an operating fluid to ambient air was performed. Considering part of the heat transfer in cooling towers is by conductive heat transfer and in terms of the low conductivity of water, it is reasonable to replace the working fluid with a fluid with higher conductivity and lower heat capacity. Recently, some studies have investigated the use of nanofluids in cooling towers. Nanofluids containing carbon nanoparticles such as carbon nanotubes and graphene performed best in the experiments. However, the stability of nanofluids containing carbon nanotubes and a water base stabilized by a surfactant is challenging. On the other hand, the use of surfactants weakens the thermal performance of nanoparticles and in some cases increases the evaporation rate by reducing the surface tension of water. Therefore, the use of functionalized carbon nanotubes, which have good stability in water without the use of surfactants, can be a good choice to improve the performance of operating fluid and thus the performance of the cooling tower with lower evaporation and water loss rates. In this study, the performance of a cross-flow wet cooling (CFWCT) tower was evaluated using four types of operating fluids including water, MWCNTs, MWCNTs-COOH, and MWCNTs-OH. The evaporation rates and process lost water for functionalized and conventional carbon nanotubes were measured and compared. The effects of the concentration of all three nanofluids on the evaluation factors of cooling tower performance such as temperature drop, efficiency, and performance characteristics were evaluated and compared. The best type of nanofluid was selected to improve the CFWCT performance.

2. Material and method

Thermophysical parameters such as thermal conductivity and convective heat transfer coefficient of nanofluids improve significantly compared to base fluids with MWCNT [47]. For instance, compared to the base fluid, the use of MWCNT nanoparticles improves the thermophysical properties of the nanofluid by 1–9 times and the heat transfer rate by 1–3 times. In addition, the effective thermal conductivity and dynamic viscosity depend on the Brownian motion of the nanoparticles [48].

Furthermore, in evaluating the heat transfer properties of cooling systems, MWCNT nanofluids are approximately five times more useful than other conventional materials [39]. Consequently, the improved thermal properties of MWCNT nanofluids influence the development of heat transfer rate and thermal efficiency of devices [48,49].

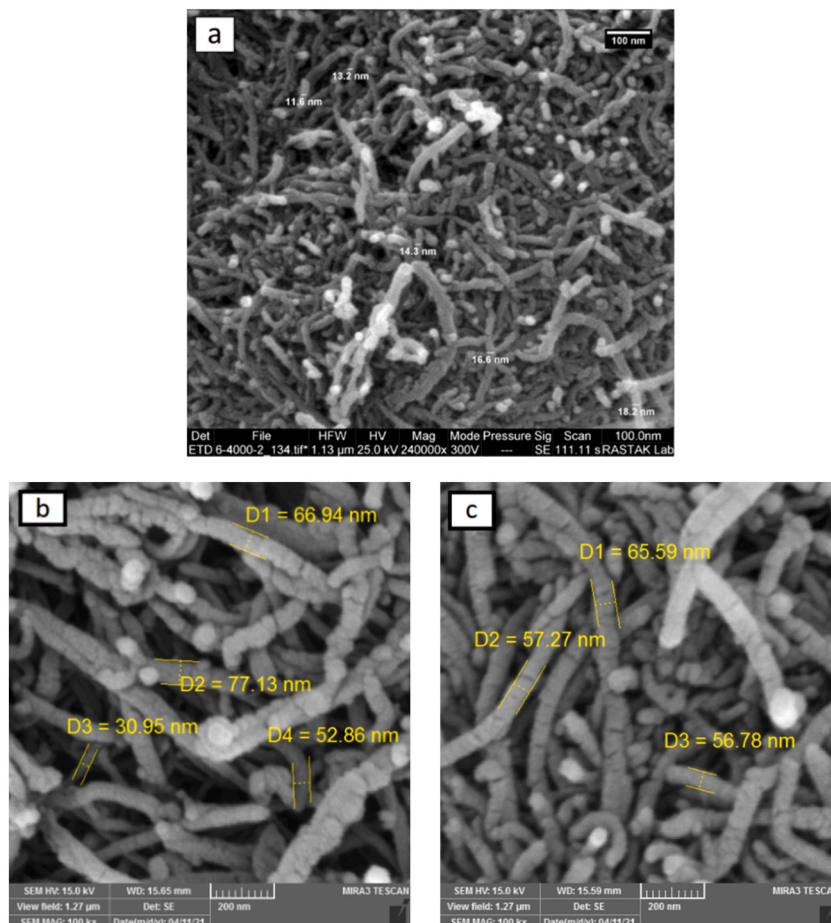


Fig. 1. SEM images of a) MWCNTs, b) MWCNTs-OH c) MWCNTs-COOH.

2.1. Preparation and characterization of nanofluid

MWCNTs, MWCNTs-COOH, and MWCNTs-OH nanoparticles were purchased from Sigma-Aldrich. SEM images as well as the nanomaterials properties are presented Fig. 1 in and Table 1, respectively. The gum arabic surfactant was purchased from Merck, Germany.

The nanofluids were prepared by two-step method. The gum arabic was weighed in a 1:1 ratio to the MWCNTs and dissolved in 10 L of water with a mechanical stirrer at 1300 rpm for 30 min to prepare conventional MWCNTs. This step was skipped in preparing functionalized MWCNTs since they were dispersed without surfactants. Then, nanoparticles were added to the prepared solution or pure water at different concentrations (0.02, 0.04, 0.06, 0.08, and 0.1 wt%). The prepared nanofluid was sonicated in an ultrasonic bath for 4 h after being stirred with a mechanical stirrer at 1300 rpm for 3 h. The nanofluids preparation steps are exhibited in Fig. 2. A visual stability test was performed to investigate the stability of the prepared nanofluids. Fig. 3 shows the result of the performed stability test of the nanofluids MWCNTs, MWCNTs-COOH and MWCNTs-OH after one day, 3 days, one week, and one month.

Dynamic light scattering (DLS) analysis is a physical method to determine the size distribution of particles in solutions and suspensions, which not only analyzes the number of particles in each dimension, but also calculates the size of the particles. The average size of interconnected nanoparticles for nanofluids containing MWCNTs-COOH, MWCNTs-OH and MWCNTs nanoparticles was approximately 35–100 nm. Because nanoparticles tend to agglomerate at higher concentrations, the diameter of nanoparticles in the base fluid rises as the number of nanoparticles added to the base fluid increases. Comparing of the results showed that the functionalized nanoparticles (MWCNTs-COOH and MWCNTs-OH) had a smaller size distribution than the MWCNTs nanoparticles in the base fluid (water). As the diameter of the nanoparticles increases, the stability of nanofluid decreases, the stability of prepared nanofluid samples shows the same results.

The dynamic light scattering (DLS) diagram of the nanofluids MWCNTs-COOH/H₂O, MWCNTs-OH/H₂O, and MWCNTs/H₂O with 0.1 wt% nanoparticles is shown in Fig. 4. The DLS test for nanofluids was performed after the preparation of the nanofluids (before the test) and after the test to determine if the nanofluid maintained its characteristics after the cycle.

DLS analysis was used to assess the nanofluids MWCNTs-COOH/H₂O, MWCNTs-OH/H₂O, and MWCNTs/H₂O, illustrating the change in the size of nanoparticle aggregations at 25 °C after the preparation of the nanofluids (before the test) and after the test to determine if the nanofluid maintained its characteristics after the cycle. The most concentrated sample of MWCNT and TiO₂ nanofluids (0.1 wt%) was selected as the sample most prone to instability. It can be derived from Fig. 4 that the change in the size distribution of the nanoparticles in all nanofluids was not very significant before and after the test, indicating maintaining the stability of the nanofluid during the process.

Table 2 illustrates the average nanoparticle size distribution and zeta potential of the nanofluids at their natural pH according to Fig. 4. The average nanoparticle size distribution also showed that the particle size distribution for MWCNTs-COOH, MWCNTs-OH and MWCNTs nanofluids hardly changed over the process.

The stabilization theory states that when the zeta potential is high (positive or negative), the electrostatic repulsions between particles increase, resulting in good suspension stability. Since the contact is opposite, particles with a high surface charge do not agglomerate. The generally accepted zeta potential values were summarized by Ghadimi et al. [50]. The zeta potential is commonly used to index the extent of electrostatic interaction between colloidal particles. It can therefore be considered a measure of the colloidal stability of the solution [51]. The zeta potential results for MWCNTs-COOH, MWCNTs-OH and MWCNTs nanofluids confirmed an average value of about 44, 42, and 33 respectively, before the test. Meanwhile, the outputs for the nanofluids after the experiments were about 45, 41 and 34 respectively, indicating sustainable stability of all suspensions during the cycle. In summary, it is worth mentioning that all nanofluids were stable before and after the experiments were performed.

The density of the nanofluids in all five concentrations prepared was measured and compared before and after the experiments to confirm that the weight percentage of nanoparticles remained constant after the experiment. The results are listed in Table 3. Due to the evaporation that took place in the system and was replaced by water, the density of the nanoparticles did not change noticeably before and after the experiments. To clarify, at lower concentrations the density of the nanofluids was the same before and after the experiment, while at higher concentrations it was slightly lower. The cause is likely because some of the nanofluids were replaced by pure water after becoming trapped in the dead zones of the filled bed or water distribution system. Inferring a constant total concentration of circulating fluid during the experiment is possible from the findings that the density of the nanofluids remained roughly constant both before and after the experiment. This is because the weight of the nanoparticles per unit volume of fluid also remained constant.

Since the thermophysical properties of the nanofluid strongly depend on the particle concentration and stability, the sustainability of thermophysical properties such as conductivity during the process can be one of the results.

Table 1
Properties of nanomaterials.

Nanomaterial	MWCNTs	MWCNTs-COOH	MWCNTs-OH
Color	Black	Black	Black
Purity	>99%	>99%	>99%
Average diameter (nm)	15	55–65	50–80
Morphology	Multi-walled hollow tubes	Multi-walled hollow tubes	Multi-walled hollow tubes
Special area (m ² /g)	>200	>200	>200
Density (g/cm ³)	2.1	2.1	2.1

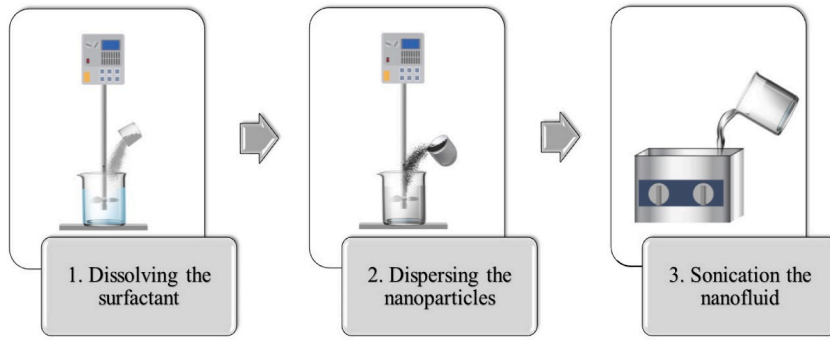


Fig. 2. The nanofluids preparation steps.

2.2. Experimental setup

The schematic diagram and components of experimental CFWCT are illustrated in Fig. 5. Also, an exterior view of the assembled experimental cross-flow wet cooling tower is depicted in Fig. 6. The heating tank has the dimensions (40 * 13 * 30 cm³) on which the other heating components were installed. The hot fluid leaving the heating tank is transferred to the upper part of the tower by a centrifugal pump. After passing via filled bed, the temperature drops and moves to the bottom of the tower. The fluid at the bottom of the tower re-enters the heating tank after the cooling cycle, heats up which is again conveyed to the upper part of the tower. This cycle continues until the process reaches steady state. A pressurized water distribution system is designed and built to achieve a more uniform distribution of the hot fluid on the filled bed. To induce air flow and direct it through the filled bed, an axial fan was installed at the exit of the tower. The filled bed plays an important role to increase the heat and mass transfer and improving the efficiency of the tower.

In this setup, a kind of splash-filled bed (mesh) was used, which is shown in Fig. 7. An aluminum droplet eliminator was added in the intake path of the fan to prevent water droplets from floating into the air and entering the ambient. During the procedure, the evaporated water must be refilled. For this purpose, a water stream with a flow rate equal to the evaporation rate in the tower, called make-up water, was used. Resistance thermocouples (RTD) type Pt-100 were installed to measure the temperatures (dry and wet bulb temperatures at the inlet and outlet, temperatures of the hot inlet and cold outlet fluid, the temperature of the fluid inside the heater and the temperature of the fluid in different parts of the bed).

In addition, the technical specifications of the instrument or device used to collect the reading and measurement are listed in Table 4.

3. Formulation

This section contains equations for some critical cooling tower parameters such as evaporation rate, temperature drop, efficiency, and performance characteristics (PC).

The theoretical evaporation rate can be specified using following equation [52]:

$$M = K(X_o - X_i) \tag{1}$$

The specific humidity of air at the outlet and inlet of the CFWCT is represented in this equation by X_o and X_i, respectively and K is the Air flow rate. In this CFWCT, the measured evaporation rate is obtained as follows:

$$M_{ev} = \frac{0.0521\Delta h_{make\ up} - 0.0429\Delta h_{heater}}{t} \tag{2}$$

Where Δh_{heater} , $\Delta h_{make\ up}$, t, are respectively the change of water level in the heating tank, the change of water level in the makeup tank, and the time to measure the evaporation rate. The water level in the heating tank must remain constant throughout the test, and the change of the water level is in terms of minor changes of the water level in the heating tank during the measurement interval.

The temperature drop (ΔT), defined as the temperature difference between hot inlet fluid ($T_{w,i}$) and cold outlet fluid ($T_{w,o}$), is calculated using following equation [24].

$$\Delta T = T_{w,i} - T_{w,o} \tag{3}$$

The efficiency of CFWCT (ϵ) is calculated by Equation (4), which is defined as the ratio of the temperature difference between cold and hot fluid to the maximum possible temperature difference [24].

$$\epsilon = \frac{T_{w,i} - T_{w,o}}{T_{w,i} - T_{a,wet,i}} \tag{4}$$

Where $T_{a,wet,i}$ is the wet bulb temperature of the entering air (ambient), $T_{w,o}$, is the temperature of the exiting fluid, and $T_{w,i}$ is the temperature of entering fluid.

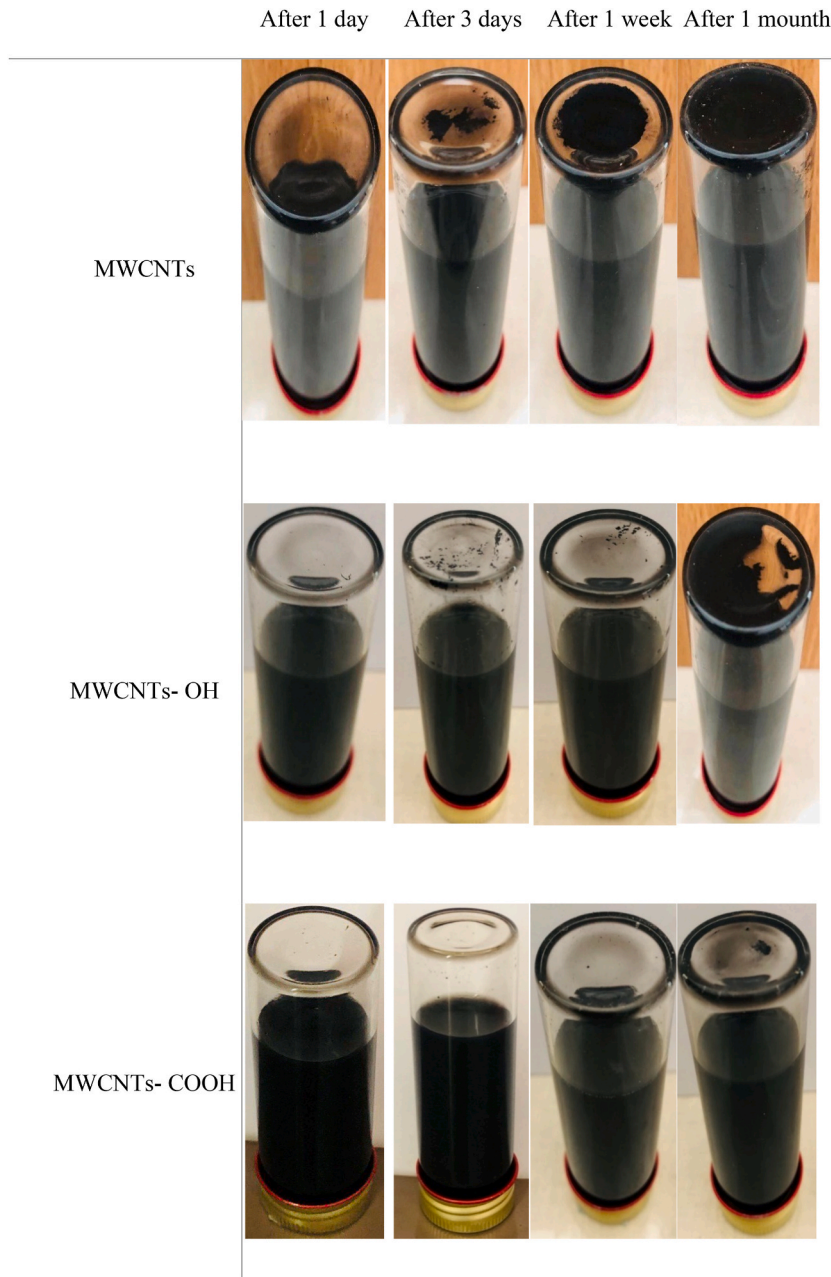


Fig. 3. Visual stability test of the nanofluids.

The CFWCT performance characteristic (PC) used to evaluate the thermal performance of the fill is defined as follows [53]:

$$PC = \frac{h_d a_{fi} A_{fr} L_{fi}}{m_w} = \frac{h_d a_{fi} L_{fi}}{G_w} = \int_{T_{wo}}^{T_{wi}} \frac{C_{pw} dT_w}{(I_{masw} - I_{ma})} \tag{5}$$

Where a_{fi} is the interfacial surface area between air and water per unit volume of fill zone (m^{-1}), h_d is the mass transfer coefficient (m/s), L_{fi} is the fill length (m), m_w is the mass flow rate of water (kg/s), A_{fr} is the frontal area of fill perpendicular to air flow direction (m^2), G_w is the mass velocity of water ($kg \cdot m^{-2} \cdot s^{-1}$), T_w is the temperature ($^{\circ}C$), C_{pw} is the specific heat at constant pressure ($J/kg \cdot K$), I_{ma} is the specific enthalpy of air-vapor (per kg dry air) (J/kg), I_{masw} is the specific enthalpy of saturated of air-vapor (per kg dry air) (J/kg).

PC is considered as a function of water mass flow rate (m_w), number of transferred units (NTU), and minimum evaporative capacity rate (C_{min}), and was determined by the ϵ - NTU method as follows [53]:

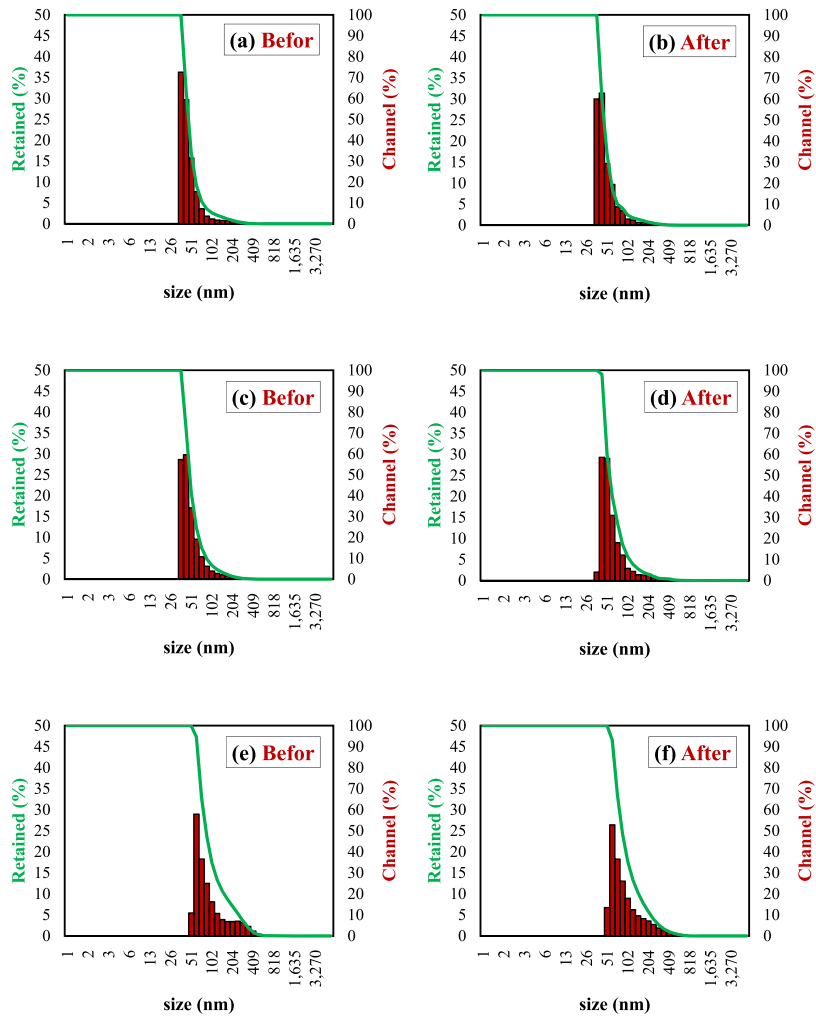


Fig. 4. DLS data analysis for the nanofluids before and after the test: a-b) MWCNTs-COOH/H₂O c-d) MWCNTs-OH/H₂O e-f) MWCNTs/H₂O.

Table 2

A summary of the zeta potential and DLS results.

Nanoparticle	Time (before or after the test cycle)	Label in Fig. 4	Average particle size distributions (nm)	Zeta potential (mV)
MWCNT-COOH	Before	a	46.2	44.2
	After	b	49.9	45.1
MWCNT-OH	Before	c	48.4	41.9
	After	d	46.8	41.6
MWCNT	Before	e	73.2	33.1
	After	f	74.6	34.7

$$PC = \frac{NTU C_{min}}{m_w} \tag{6}$$

The system of equations must be solved simultaneously using an iteration method to obtain NTU and C_{min} . This system of equations is shown below [53,54].

$$\varepsilon = \left[\frac{1}{1 - \exp(-NTU)} + \frac{C}{1 - \exp(-C.NTU)} - \frac{1}{NTU} \right]^{-1} \tag{7}$$

Table 3
Change in density of nanofluids during the cooling process.

Weight percent of nanoparticles	Time (before or after the test cycle)	MWCNTs-COOH (g/cm ³)	MWCNTs-OH (g/cm ³)	MWCNTs (g/cm ³)
0.02 wt%	Before	0.9962	0.9962	0.9962
	After	0.9962	0.9962	0.9962
0.04 wt%	Before	0.9965	0.9965	0.9965
	After	0.9965	0.9965	0.9965
0.06 wt%	Before	0.9968	0.9968	0.9967
	After	0.9967	0.9967	0.9967
0.08 wt%	Before	0.9970	0.9970	0.9969
	After	0.9969	0.9968	0.9968
0.1 wt%	Before	0.9973	0.9973	0.9971
	After	0.9971	0.9972	0.9970

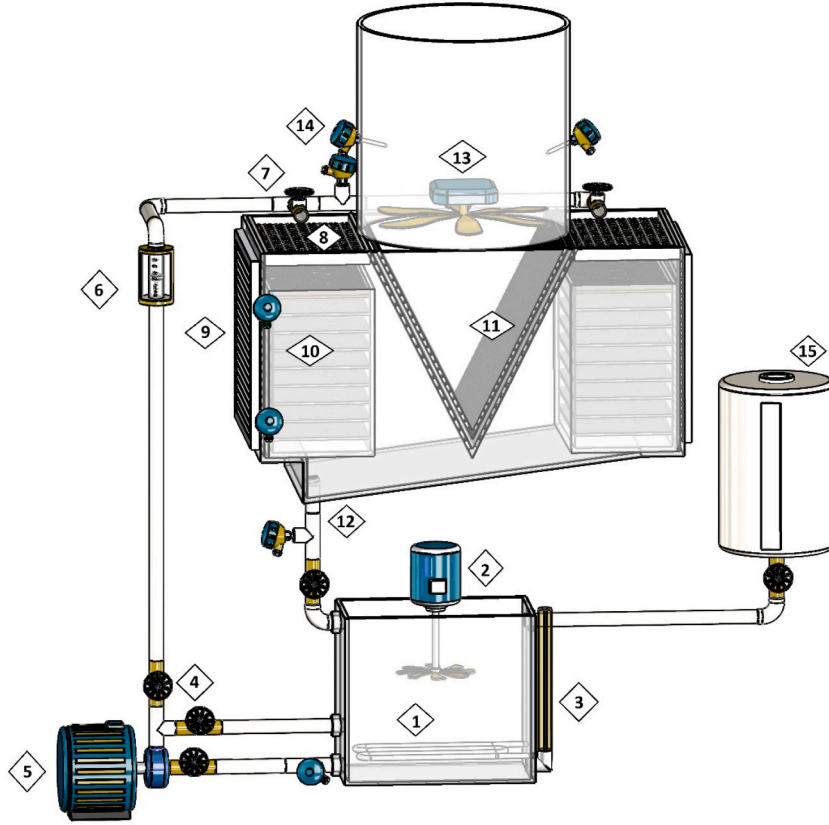


Fig. 5. Schematic of experimental setup.

$$\varepsilon = \frac{Q}{Q_{max}} \tag{8}$$

$$Q = m_a(I_{mao} - I_{mai}) \tag{9}$$

$$Q_{max} = C_{min}(I_{maswi} - I_{mai}) \tag{10}$$

$$\lambda = \frac{(I_{maswo} + I_{maswi} - 2I_{masw})}{4} \tag{11}$$

$$C_{min} = \min\left(m_w C_{pw} \frac{dI_{masw}}{dT_w}, m_a\right) \tag{12}$$

$$C_{max} = \max\left(m_w C_{pw} \frac{dI_{masw}}{dT_w}, m_a\right) \tag{13}$$



Fig. 6. Exterior view of the assembled experimental cross-flow cooling tower.

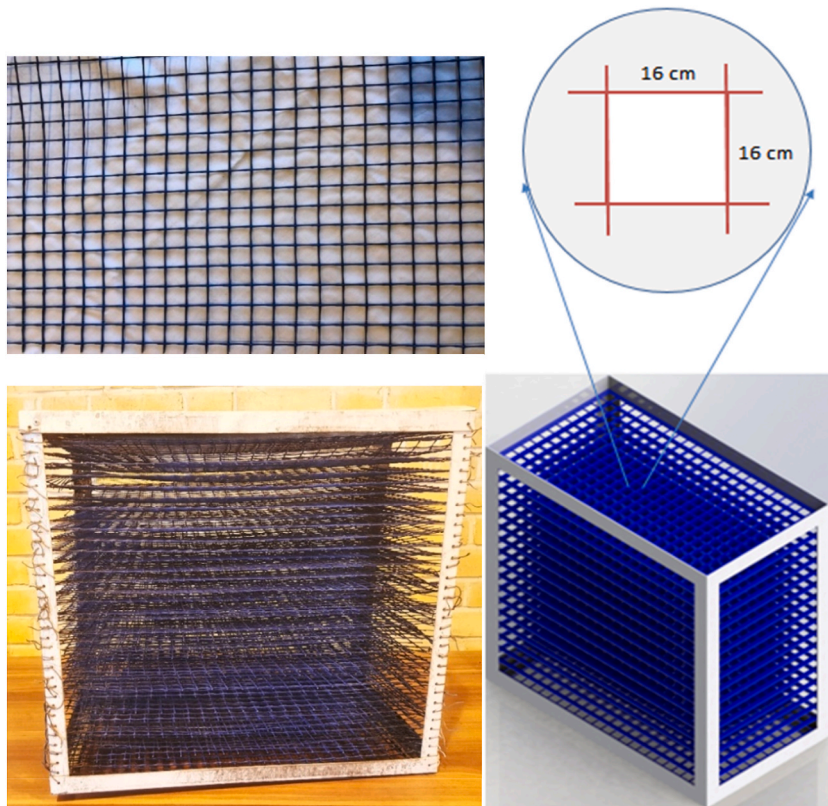


Fig. 7. The filled bed and its details.

$$\frac{dI_{masw}}{dT_w} = \frac{I_{masw} - I_{maswo}}{T_{w,i} - T_{w,o}} \quad (14)$$

Table 4
The technical specifications of the instrument.

Instrument	Model	Range	Accuracy	Application
Water flow meter	KYTOLA- A5AA Finland	0.5–6 m/s	0.5 m/s	Flow rate
Laboratory balance	GRAM- FS China	0.0001–120 g	0.0001 g	Particles weight
Temperature controller	Omron- E5CC Japan	–25 – 65 °C	0.1 °C	Temperature display
Anemometer	MASTECH- MS6252B Germany	0.8–30 m/s	0.01 m/s	Air velocity

$$C = \frac{C_{min}}{C_{max}} \tag{15}$$

In addition, the performance characteristics of tower (PC) under various operating conditions can be expressed in terms of the ratio between the flow rate of water and the air entering the tower [55].

$$PC = b \left(\frac{m}{K} \right)^{-n} \tag{16}$$

where m and K are the water and air flow rates, respectively, at the inlet. b and n are the cooling tower constants.

When the working fluid is nanofluids, Equation (17) is used to estimate the specific heat of nanofluids [56,57].

$$(\rho C_p)_{nf} = (1 - \varphi)(\rho C_p)_{bf} + \varphi(\rho C_p)_p ; (\rho)_{nf} = (1 - \varphi)(\rho)_{bf} + \varphi(\rho)_p \tag{17}$$

Where, $(C_p)_{bf}$, $(C_p)_{nf}$, and $(C_p)_p$ represent the specific heat of base fluid, the nanofluid, and nanoparticles, respectively. The volume concentration of nanofluids is φ .

4. Uncertainty analysis

Because the accuracy of the devices utilized in this investigation varied, the parameters measured with these devices had inaccuracies as well. The effect of parameter measurement error on the obtained results was assessed. The following methods were used to calculate the uncertainty of the measured parameters [65].

$$M = f(y_1, y_2, \dots, y_n) \tag{18}$$

$$U_M = \pm \left\{ \left(\frac{y_1}{M} \frac{\partial M}{\partial y_1} u_{y_1} \right)^2 + \left(\frac{y_2}{M} \frac{\partial M}{\partial y_2} u_{y_2} \right)^2 + \dots + \left(\frac{y_n}{M} \frac{\partial M}{\partial y_n} u_{y_n} \right)^2 \right\}^{1/2}$$

Where y_i denotes the measurable parameter, u_{yi} the measured error, and U_M the maximum error of the parameter M . The maximum error of measured quantities is shown in Table 5.

5. Results and discussion

The effect of nanofluids MWCNTs/H₂O, MWCNTs-COOH/H₂O, and MWCNTs-OH/H₂O was evaluated using a square splash bed in a CFWCT under nearly constant operating and ambient conditions (ambient temperature about 26 °C, inlet water flow rate of 3 kg/min, and air flow rate of 8 kg/min). All three nanofluids were prepared at 5 different concentrations of 0.02 wt%, 0.04 wt%, 0.06 wt%, 0.08 wt% and 0.1 wt%. Experiments were performed once with pure water and once with different concentrations of nanofluids. The results were recorded when the process reached steady state.

Table 5
The maximum uncertainty in the obtained characteristics.

Characteristics	Maximum inaccuracy (%)
Efficiency (ε)	0.9
Weight fraction (wt)	0.5
Temperature drop	0.4
Water Mass flow rate	3
Evaporation rate	0.4
Temperature (°C)	0.05
Air mass flow rate	0.3
Mass of nanoparticle (m _{np})	0.5

5.1. Effect of nanofluid concentration on evaporation rate

Latent heat of evaporation plays an important role to lower water temperature in cooling towers. When the water evaporation rate in a cooling tower is higher, the thermal performance of tower improves.

Fig. 8(a), (b), and (c) compare the theoretical and measured evaporation rates of MWCNTs-COOH/H₂O, MWCNTs-OH/H₂O, and MWCNTs/H₂O nanofluids. At all concentrations, nanofluids had approximately similar results at all concentrations and showed acceptable agreement between the theoretical and measured evaporation rates. This was a proof of the accuracy of the information obtained from the experiments. In all experiments conducted, the theoretical evaporation rates were slightly lower than the measured evaporation rates. This was in terms of the low evaporation from the heating tank, which could not be measured.

A comparison between functionalized (MWCNTs-COOH/H₂O and MWCNTs-OH/H₂O) and conventional MWCNTs/H₂O nanofluids is illustrated in Fig. 9(a). The evaporation rate of MWCNTs-COOH/H₂O and MWCNTs-OH/H₂O nanofluids decreased with increasing concentration. However, the evaporation rate of MWCNTs/H₂O increased by increasing concentration. This is because a surfactant was used for the stabilization in preparing the MWCNTs/H₂O nanofluid, reducing the nanofluid's surface tension, thereby increasing the evaporation rate. The nanofluids prepared with functionalized carbon nanotube nanoparticles (MWCNTs-COOH/H₂O and MWCNTs-OH/H₂O) are sufficiently stable in water without using a surfactant. The stability of carbon nanotube nanoparticles in water is enhanced by the covalent functionalities of carboxyl and hydroxyl groups.

In MWCNTs-COOH/H₂O nanofluid, the evaporation rate decreased by increasing concentration, the highest evaporation rate was 71.7% at 0.01 wt%. The evaporation rate reduced at a concentration of 0.08 wt% in MWCNTs-OH/H₂O nanofluid and the concentrations from 0.08 wt% to 0.1 wt% the evaporation rate slightly increased. For MWCNTs/H₂O nanofluid, the evaporation rate was slightly higher than for water at all concentrations, which can be in terms of the presence of surfactant in the nanofluid. In some cases, using the surfactants to stabilize nanofluids reduces the surface tension, and thus the enthalpy of evaporation, which increases the evaporation rate [59–61].

Fig. 9(a) shows the evaporation rates of water and nanofluids at different concentrations. As well as, the percent change in the evaporation rates of nanofluids in the tower compared to water at different concentrations is shown in Fig. 9(b). The change in the evaporation rate of MWCNTs-COOH/H₂O and MWCNTs-OH/H₂O nanofluids was negative compared to water. This is because the nanoparticles in the nanofluids decrease the vapor pressure and thus the evaporation rate. In contrast, the change in the evaporation rate of MWCNTs/H₂O nanofluids was positive compared to pure water. The percent change in evaporation rate by functionalized carbon nanotube nanoparticles was very similar. The highest change was due to the MWCNTs-COOH/H₂O nanofluid at a concentration of 0.1 wt%, which corresponds to -4.2% compared to water. However, at the same concentration of MWCNTs/H₂O nanofluid, the evaporation rate increased by 1.4% compared to water. Thus, one of the positive effects of using functionalized nanotube nanoparticles compared to conventional carbon nanotubes stabilized by surfactants was reducing evaporation rate and lower water consumption in CFWCT.

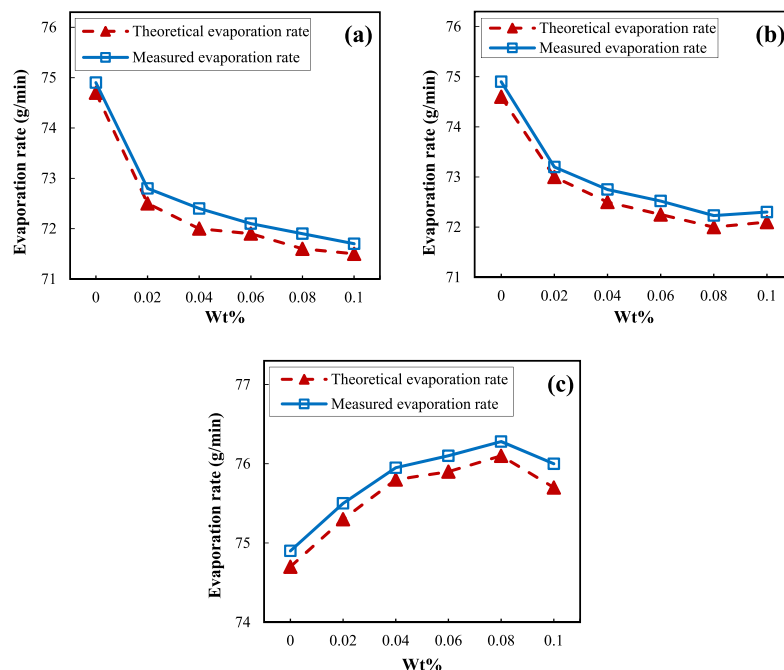


Fig. 8. Comparison of measured and theoretical evaporation rates of nanofluids at different concentrations: (a) MWCNTs-COOH/H₂O, (b) MWCNTs-OH/H₂O, and (c) MWCNTs.

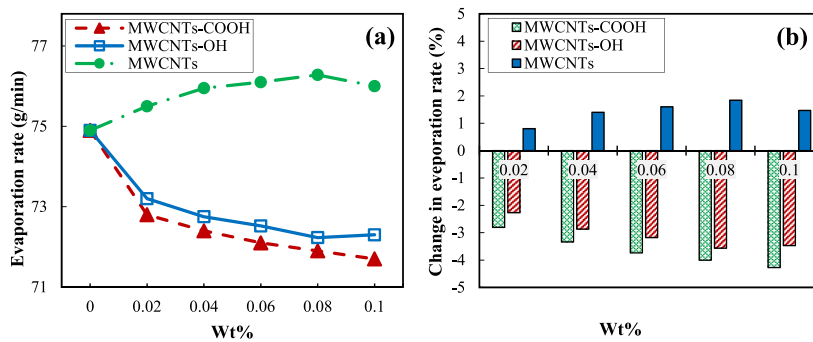


Fig. 9. Evaporation rate comparison: (a) Evaporation rates of various nanofluids at different concentrations and (b) Percentage changes in evaporation rates of various nanofluids in the tower compared to water at different concentrations.

5.2. Effect of nanofluid concentration on cooling performance characteristics (PC)

The characteristics of the tower is one of the most important and significant parameters in the analysis of the cooling tower performance [23].

The performance characteristics of CFWCT was calculated by the system of equations (5- 17) for different concentrations of nanofluids. Fig. 10(a) exhibits the results of all nanofluids and Fig. 10(b) compares the performance characteristics of the CFWCT utilizing nanofluids compared to pure water. The performance of the CFWCT with MWCNTs-COOH/H₂O nanofluid was improved by increasing the concentration. The addition of MWCNTs-COOH/H₂O to pure water improved the performance characteristic of the CFWCT at all concentrations, and the highest characteristic value of the tower was equal to 0.338 at a concentration of 0.1 wt%. The graph's steepest slope was found in the concentration range of 0 wt% to 0.02 wt%. The performance characteristic of the tower altered with a softer slope as the concentration was raised above 0.02 wt%. Moreover, the performance characteristics of CFWCT with MWCNTs-OH/H₂O nanofluid were lower than those of the tower with MWCNTs-COOH/H₂O nanofluid. At a concentration of 0 wt% to 0.08 wt%, the CFWCT performance increased and then decreased from a concentration of 0.08 wt% to 0.1 wt%. On the other hand, the characteristics of the CFWCT depend on the fluid flow, the dimensions of the tower, and the mass and heat transfer coefficients. In the case study, the fluid flow and the dimensions of CFWCT were constant. Thus, the improvement in the characteristics of the CFWCT is in terms of the enhancement in the mass and heat transfer coefficients. MWCNTs/H₂O nanofluids indicated the lowest performance characteristics compared to functionalized carbon nanotube nanofluids (MWCNTs-COOH/H₂O and MWCNTs-OH/H₂O). The difference in the performance characteristics of CFWCT is due to the lower stability of the MWCNTs/H₂O nanofluid compared to the other two nanofluids, which not only reduces the heat and mass transfer coefficients, but also weakens the performance of the CFWCT. Up to a concentration of 0.06 wt% MWCNTs/H₂O nanofluid, the characteristics of tower improved and then started to decrease. The highest characteristic of the tower with MWCNTs/H₂O nanofluid was 0.316. According to Fig. 10(a), the obtained performance characteristics with nanofluids were better than with pure water at all concentrations of the nanofluids. The highest percent changes in MWCNTs-COOH/H₂O nanofluid were 17.1%, in MWCNTs-OH/H₂O nanofluid 11.7%, and in MWCNTs/H₂O nanofluid 8.2%, compared with pure water. In the nanofluids, MWCNTs-OH/H₂O and MWCNTs/H₂O with a concentration of 0.08 wt%, the characteristics of CFWCT were reduced. The reduction in the characteristics of the tower in the MWCNTs nanofluid was greater than in the MWCNTs-OH/H₂O. In other words, when the concentration of nanofluids was increased by 0.02 wt% (0.08 wt% to 0.1 wt%), the cooling performance characteristics of the CFWCT decreased by 0.6% with MWCNTs-OH/H₂O nanofluid, while it fell more than 2% with the MWCNTs nanofluid.

5.3. Effect of nanofluid concentration on the temperature drop of CFWCT

Equation (3) was used to calculate the temperature drop of CFWCT for water and different concentrations of the nanofluids, MWCNTs/H₂O, MWCNTs-COOHs/H₂O, and MWCNTs-OH/H₂O; the results are shown in Fig. 11(a). Fig. 11(b) indicates the temperature drop of the tower for each nanofluid compared to the temperature drop of water. The temperature drop of the tower rose as the concentration of MWCNTs-COOH/H₂O nanofluid increased, as shown in Fig. 11(a). Regarding the proximity of the concentrations studied, the increase exhibited a gentle slope. The temperature drop of CFWCT utilizing MWCNTs-OH/H₂O nanofluid was divided into three parts. It increased from 0 wt% to 0.06 wt%, was nearly constant from 0.06 wt% to 0.08 wt%, and exhibited an approximately decreasing trend from 0.08 wt% to 0.1 wt%. For MWCNTs/H₂O nanofluid, the temperature drop of the CFWCT increased from 0 to 0.06 wt% and decreased from 0.06 wt% to 0.1 wt%. The slope of the decrease in the temperature drop from 0.08 to 0.1 wt% was larger than that at 0.06 to 0.08 wt%.

For all concentrations of nanofluids, the largest increase in the temperature drop was found in a concentration range from 0 wt% to 0.02 wt%. This is due to the fact that the addition of carbon nanotubes to water affects the thermal conductivity of the CFWCT. On the other hand, the heat capacity of nanofluid is lower than that of water. Therefore, by the same energy input by the element, it led to a further increase in the temperature of the inlet fluid, which eventually increased the temperature drop of CFWCT.

As the temperature drop of CFWCT increases, the cooling capacity of the tower increases, which means that the thermal

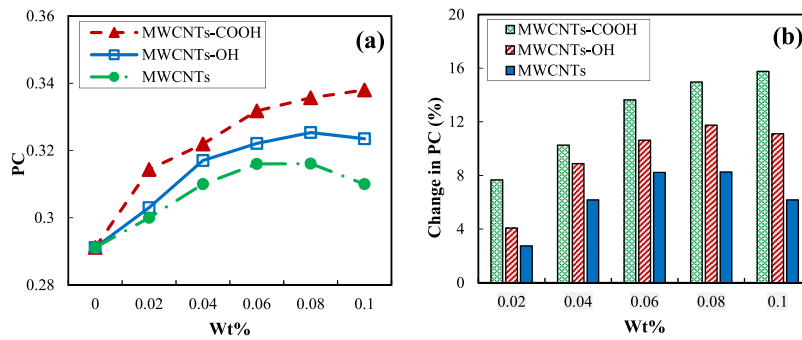


Fig. 10. Performance characteristics: (a) Using nanofluids at different concentrations and (b) Percentage changes using nanofluids compared to water at different concentrations.

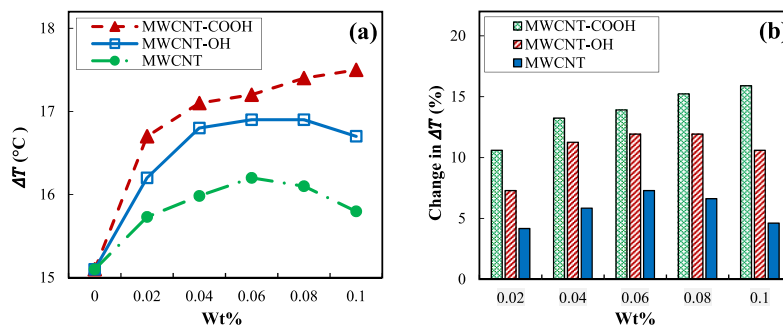


Fig. 11. Temperature drop: (a) At different concentrations and (b) Percentage changes using nanofluids compared to water at different concentrations.

performance of the tower has improved. Brownian motion, i.e. the irregular and random movement of particles, is one of the decisive factors in the heat transfer of nanofluids. Brownian motion only occurs when there are very small particles in the fluid, so the effect of Brownian motion disappears with increasing particle size. In addition, nanoparticles significantly increase the transfer surface and convective heat transfer coefficient, which in turn improves heat transfer in nanofluids [62–64]. Thus, by increasing the conductive and convective heat transfer and reducing the heat capacity of nanofluids compared to the base fluid, the use of nanofluids improves the heat transfer in the cooling tower and consequently increases the temperature drop and cooling capacity. According to Fig. 11(b), among all nanofluids, MWCNTs-COOH/H₂O had the highest cooling capacity of the CFWCT compared to water, 15.89% at 0.1 wt%. For the nanofluids (MWCNTs- OH/H₂O and MWCNTs/H₂O), the highest temperature drop was 11.9% and 7.28%, respectively, corresponding to 0.06 wt%. The difference may be explained by the fact that functionalized carbon nanotubes (without surfactant) have a higher stability than conventional carbon nanotubes.

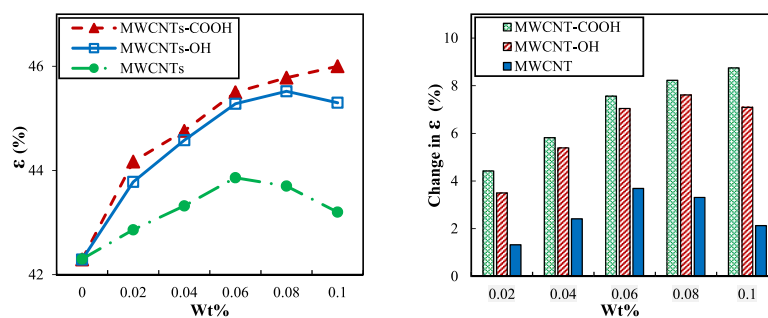


Fig. 12. Efficiency: (a) At different concentrations and (b) Percentage changes using nanofluids compared to water at different concentrations.

5.4. Effect of nanofluid concentration on CFWCT efficiency

The efficiency of CFWCT was calculated using equation (4) for different concentrations of MWCNTs-COOH/H₂O, MWCNTs-OH/H₂O, and MWCNTs/H₂O nanofluids. The results are compared in Fig. 12(a) and the percent change compared to pure water is shown in Fig. 12(b). As Fig. 12(a) shows, as the concentration increased in all nanofluids, the efficiency of the tower improved compared to pure water. The highest efficiency of tower was observed with the nanofluid MWCNTs-COOH/H₂O at a concentration limit of 0 wt% to 0.02 wt%. The efficiency had a smoothly increasing trend in terms of the proximity of the concentrations studied. The efficiency of MWCNTs-OH/H₂O nanofluid was very similar to that of the MWCNTs-COOH/H₂O. At 0.08 wt% to 0.1 wt%, the efficiency of CFWCT was lower than that of MWCNTs-COOH/H₂O when MWCNTs- OH/H₂O nanofluid was used. As the concentration increases, the probability of nanoparticle agglomeration increases.

The difference in the efficiency of CFWCT with functionalized and conventional carbon nanotube nanofluids is indicated in Fig. 12 (a). The highest efficiency of the CFWCT with MWCNTs/H₂O nanofluid was 43.86% at a concentration of 0.06%, while the maximum efficiency of the CFWCT with MWCNTs-COOH/H₂O and MWCNTs- OH/H₂O nanofluids was about 46%. Due to the stability difficulty of the MWCNTs/H₂O nanofluid, the efficiency of the CFWCT fell from 0.06 wt% to 0.1 wt%. Despite a drop in efficiency, the CFWCT was still more efficient than pure water.

Fig. 12(b) dedicates that the efficiency of nanofluids increased at all concentrations compared to pure water. For all nanofluids, the lowest efficiency compared to water was at a concentration of 0.02 wt%, but the highest efficiency was different in terms of the effect of nanofluid stability. Compared to pure water, the maximum change in the efficiency of MWCNTs-COOH/H₂O nanofluid was 8.74% at 0.1 wt% and the lowest value was 4.42% at 0.02 wt%. moreover, the largest and lowest change in the efficiency of CFWCT with MWCNTs-OH/H₂O nanofluid compared to pure water was 7.6% at 0.08 wt% and 3.4% at 0.02 wt%, respectively. For MWCNTs/H₂O nanofluid, the maximum and minimum were 3.68% at 0.06 wt% and 1.32% at 0.02 wt%, respectively.

6. Conclusion

In this study, three nanofluids MWCNTs/H₂O, MWCNTs-COOH/H₂O, and MWCNTs- OH/H₂O were substituted as working fluids instead of water in a laboratory CFWCT. The effects of three nanofluids on the critical operating factors of the CFWCT such as evaporation rate, performance characteristics, temperature drop, and tower efficiency were evaluated. In addition to the effect of the operating fluid type on the thermal performance of the CFWCT, the concentration effect of the individual nanofluids was analyzed. The following is a summary of some of the key findings:

- Despite using gum arabic as a surfactant to stabilize the MWCNTs/H₂O nanofluids, the results of the visual stability test and DLS showed that the stability of the functionalized nanofluids, MWCNTs-COOH/H₂O and MWCNTs- OH/H₂O, was better than that of the non-functionalized nanofluid.
- Regardless of the type of nanofluid, adding a small amount of nanoparticles to the base fluid (water) improved CFWCT performance compared to water.
- Evaporation rates with MWCNTs/H₂O nanofluid are increased compared to water. While using MWCNTs-COOH/H₂O and MWCNTs- OH/H₂O nanofluids decreased the evaporation rate compared to water despite the better thermal performance of the tower.
- As the concentration of nanofluids increased, the factors determining the thermal performance of tower always indicated an upward trend for MWCNTs-COOH/H₂O nanofluids, while they increased up to 0.06 wt% and 0.08 wt% for MWCNTs/H₂O and MWCNTs-OH/H₂O nanofluids, respectively. The upward trend then stopped with increasing concentration. The decreasing stability with increasing concentration may be one of the factors affecting the result.
- The percent improvement in tower performance characteristics with MWCNTs/H₂O, MWCNTs-COOH/H₂O, and MWCNTs-OH/H₂O nanofluids at 0.1 wt% compared to water was 6.17%, 15.85, and 11.1%, respectively.
- The major limitations of using nanofluids in the cooling tower were determined to be dead zones within the filled bed and the trapping of the nanofluid, resulting in its sedimentation in parts of the tower. Sediment transport by the working fluid can cause parts of the cooling tower, such as the water distribution system, to become blocked over time. Therefore, the use of nanofluids with higher concentrations that tend to agglomerate was avoided in this research to prevent changes in the concentration of circulating nanofluids and clogging.
- The effects of nanofluid properties, such as thermal conductivity, viscosity, stability, and vaporization temperature, can be considered in the following studies.

Author contribution

Nazanin Karimi Bakhtiyar: Investigation, Methodology, Formal analysis, Writing original draft. **Reza Javadpour:** Formal analysis, Writing original draft. **Saeed Zeinali Heris:** Supervision, Validation, Formal analysis, Review & Editing. **Mousa Mohammadpourfard:** Formal analysis.

Declaration of competing interest

The authors declare that they have no known competing financial interests or personal relationships that could have appeared to influence the work reported in this paper.

Data availability

No data was used for the research described in the article.

References

- [1] J. Ruiz, P. Navarro, M. Hernández, M. Lucas, A.S. Kaiser, Thermal performance and emissions analysis of a new cooling tower prototype, *Appl. Therm. Eng.* (2022) 206, <https://doi.org/10.1016/j.applthermaleng.2022.118065>.
- [2] H. Hanif, S. Shafie, Interaction of multi-walled carbon nanotubes in mineral oil based Maxwell nanofluid, *Sci. Rep.* 12 (2022) 4712, <https://doi.org/10.1038/s41598-022-07958-y>.
- [3] X. Fan, X. Lu, H. Nie, H. Zhu, Q. Wang, Y. Kang, S. Liu, X. Zheng, Z. Liu, Y. Zhang, X. Long, J. Li, An experimental study of a novel dew point evaporative cooling tower based on M-cycle, *Appl. Therm. Eng.* 190 (2021), 116839, <https://doi.org/10.1016/J.APPLTHERMALENG.2021.116839>.
- [4] X. Li, F. Sun, X. Chen, C. Liu, Impact mechanism of the chip muffler layout patterns on the cooling performance of wet cooling towers, *Appl. Therm. Eng.* (2019) 161, <https://doi.org/10.1016/j.applthermaleng.2019.114058>.
- [5] N.P. Chermisinoff, P.N. Chermisinoff, *Cooling Towers : Selection, Design, and Practice*, 1981, p. 347.
- [6] R.F.F. Pontes, W.M. Yamauchi, E.K.G. Silva, Analysis of the effect of seasonal climate changes on cooling tower efficiency, and strategies for reducing cooling tower power consumption, *Appl. Therm. Eng.* 161 (2019), 114148, <https://doi.org/10.1016/j.applthermaleng.2019.114148>.
- [7] D. Lyu, F. Sun, Y. Zhao, Impact mechanism of different fill layout patterns on the cooling performance of the wet cooling tower with water collecting devices, *Appl. Therm. Eng.* 110 (2017) 1389–1400, <https://doi.org/10.1016/J.APPLTHERMALENG.2016.08.190>.
- [8] A.V. Dmitriev, I.N. Madyshv, V.v. Kharkov, O.S. Dmitrieva, V.E. Zinurov, Experimental investigation of fill pack impact on thermal-hydraulic performance of evaporative cooling tower, *Therm. Sci. Eng. Prog.* 22 (2021), 100835, <https://doi.org/10.1016/J.TSEP.2020.100835>.
- [9] A. Ayoub, B. Gjorgiev, G. Sansavini, Cooling towers performance in a changing climate: techno-economic modeling and design optimization, *Energy* 160 (2018) 1133–1143, <https://doi.org/10.1016/J.ENERGY.2018.07.080>.
- [10] D. Pandelidis, Numerical study and performance evaluation of the Maisotsenko cycle cooling tower, *Energy Convers. Manag.* 210 (2020), 112735, <https://doi.org/10.1016/J.ENCONMAN.2020.112735>.
- [11] J.H. Yu, Z.G. Qu, J.F. Zhang, S.J. Hu, J. Guan, Comprehensive coupling model of counter-flow wet cooling tower and its thermal performance analysis, *Energy* 238 (2022), 121726, <https://doi.org/10.1016/J.ENERGY.2021.121726>.
- [12] W. Wang, H. Zhang, P. Liu, Z. Li, J. Lv, W. Ni, The cooling performance of a natural draft dry cooling tower under crosswind and an enclosure approach to cooling efficiency enhancement, *Appl. Energy* 186 (2017) 336–346, <https://doi.org/10.1016/j.apenergy.2016.02.007>.
- [13] S.B. Mousavi, S. Zeinali Heris, M.G. Hosseini, Experimental investigation of MoS₂/diesel oil nanofluid thermophysical and rheological properties, *Int. Commun. Heat Mass Tran.* 108 (2019), 104298, <https://doi.org/10.1016/J.JICHEATMASSTRANSFER.2019.104298>.
- [14] H. Alizadeh, H. Pourpasha, S. Zeinali Heris, P. Estellé, Experimental investigation on thermal performance of covalently functionalized hydroxylated and non-covalently functionalized multi-walled carbon nanotubes/transformer oil nanofluid, *Case Stud. Therm. Eng.* 31 (2022), <https://doi.org/10.1016/j.csite.2021.101713>.
- [15] H. Pourpasha, S. Zeinali Heris, Y. Mohammadfam, Comparison between multi-walled carbon nanotubes and titanium dioxide nanoparticles as additives on performance of turbine meter oil nano lubricant, *Sci. Rep.* 2021 11 (2021) 1–11, <https://doi.org/10.1038/s41598-021-90625-5>, 1–19.
- [16] S. Nejatbakhsh, H. Aghdasinia, M.E. Farshchi, B. Azimi, A. Karimi, Adsorptive desulfurization of liquid hydrocarbons utilizing granular Cu/Cr-BDC- γ -Al₂O₃ bimetal-organic frameworks, *Ind. Eng. Chem. Res.* 61 (2022) 11617–11627, <https://doi.org/10.1021/ACS.IECR.2C01491>.
- [17] M.J. Nobarzad, M. Tahmasebpour, M. Heidari, Theoretical and experimental study on the fluidity performance of hard-to-fluidize carbon nanotubes-based CO₂ capture sorbents, *Front. Chem. Sci. Eng.* (2022), <https://doi.org/10.1007/S11705-022-2159-X>.
- [18] M. Heidari, M. Tahmasebpour, A. Antzaras, A.A. Lemonidou, CO₂ capture and fluidity performance of CaO-based sorbents: effect of Zr, Al and Ce additives in tri-, bi- and mono-metallic configurations, *Process Saf. Environ. Protect.* 144 (2020) 349–365, <https://doi.org/10.1016/j.psep.2020.07.041>.
- [19] M. Heidari, M. Tahmasebpour, S.B. Mousavi, C. Pevida, CO₂ capture activity of a novel CaO adsorbent stabilized with (ZrO₂+Al₂O₃+CeO₂)-based additive under mild and realistic calcium looping conditions, *J. CO₂ Util.* 53 (2021), <https://doi.org/10.1016/j.jcou.2021.101747>.
- [20] A. Aghaei Sarvari, S. Zeinali Heris, M. Mohammadpourfard, S.B. Mousavi, P. Estellé, Numerical investigation of TiO₂ and MWCNTs turbine meter oil nanofluids: flow and hydrodynamic properties, *Fuel* (2022) 320, <https://doi.org/10.1016/j.fuel.2022.123943>.
- [21] C. Maatki, Heat transfer enhancement using CNT-water nanofluids and two stages of seawater supply in the triangular solar still, *Case Stud. Therm. Eng.* 30 (2022), 101753, <https://doi.org/10.1016/J.CSITE.2021.101753>.
- [22] H. Pourpasha, P. Farshad, S. Zeinali Heris, Modeling and optimization the effective parameters of nanofluid heat transfer performance using artificial neural network and genetic algorithm method, *Energy Rep.* 7 (2021) 8447–8464, <https://doi.org/10.1016/J.EGYR.2021.10.121>.
- [23] P. Imani-Mofrad, Z.H. Saeed, M. Shanbedi, Experimental investigation of filled bed effect on the thermal performance of a wet cooling tower by using ZnO/water nanofluid, *Energy Convers. Manag.* 127 (2016) 199–207, <https://doi.org/10.1016/J.ENCONMAN.2016.09.009>.
- [24] P. Imani-Mofrad, S. Zeinali Heris, M. Shanbedi, Experimental investigation of the effect of different nanofluids on the thermal performance of a wet cooling tower using a new method for equalization of ambient conditions, *Energy Convers. Manag.* 158 (2018) 23–35, <https://doi.org/10.1016/J.ENCONMAN.2017.12.056>.
- [25] A.M. Elsaid, A novel approach for energy and mass transfer characteristics in wet cooling towers associated with vapor-compression air conditioning system by using MgO and TiO₂ based H₂O nanofluids, *Energy Convers. Manag.* 204 (2020), 112289, <https://doi.org/10.1016/J.ENCONMAN.2019.112289>.
- [26] M. Amini, M. Zareh, S. Maleki, Thermal performance analysis of mechanical draft cooling tower filled with rotational splash type packing by using nanofluids, *Appl. Therm. Eng.* 175 (2020), 115268, <https://doi.org/10.1016/J.APPLTHERMALENG.2020.115268>.
- [27] R. Javadpour, S. Zeinali Heris, J.P. Meyer, Experimental study of the effect of filled bed type on the performance of a cross-flow cooling tower with the approach of using nanofluids, *Energy Rep.* 8 (2022) 8346–8360, <https://doi.org/10.1016/J.EGYR.2022.06.027>.
- [28] R. Javadpour, S. Zeinali Heris, Y. Mohammadfam, Optimizing the effect of concentration and flow rate of water/MWCNTs nanofluid on the performance of a forced draft cross-flow cooling tower, *Energy* 217 (2021), 119420, <https://doi.org/10.1016/J.ENERGY.2020.119420>.
- [29] M. Rahmati, Effects of ZnO/water nanofluid on the thermal performance of wet cooling towers, *Int. J. Refrig.* 131 (2021) 526–534, <https://doi.org/10.1016/J.IJREFRIG.2021.03.017>.
- [30] M.M. Bhatti, H.F. Öztop, R. Ellahi, I.E. Sarris, M.H. Doranehgard, Insight into the investigation of diamond (C) and Silica (SiO₂) nanoparticles suspended in water-based hybrid nanofluid with application in solar collector, *J. Mol. Liq.* 357 (2022) 119134, <https://doi.org/10.1016/j.molliq.2022.119134>.
- [31] V. Chinnasamy, H. Cho, Investigation on thermal properties enhancement of lauryl alcohol with multi-walled carbon nanotubes as phase change material for thermal energy storage, *Case Stud. Therm. Eng.* 31 (2022), <https://doi.org/10.1016/j.csite.2022.101826>, 101826.
- [32] C.J. Ho, K.-Y. Liu, T.-F. Yang, S. Rashidi, W.-M. Yan, Experimental study on cooling performance of water-based hybrid nanofluid with PCM and graphene nanoparticles, *Case Stud. Therm. Eng.* 33 (2022), 101939, <https://doi.org/10.1016/j.csite.2022.101939>.
- [33] N. Ali, A.M. Bahman, N.F. Aljuwayhel, S.A. Ebrahim, S. Mukherjee, A. Alsayegh, Carbon-based nanofluids and their advances towards heat transfer applications—a review, *Nanomaterials* 11 (2021) 1628, <https://doi.org/10.3390/nano11061628>.
- [34] E.A. Chavez Panduro, F. Finotti, G. Largiller, K.Y. Lervåg, A review of the use of nanofluids as heat-transfer fluids in parabolic-trough collectors, *Appl. Therm. Eng.* 211 (2022), 118346, <https://doi.org/10.1016/j.applthermaleng.2022.118346>.
- [35] T.O. Babarinde, S.A. Akinlabi, D.M. Madyira, F.M. Ekundayo, Enhancing the energy efficiency of vapour compression refrigerator system using R600a with graphene nanolubricant, *Energy Rep.* 6 (2020) 1–10, <https://doi.org/10.1016/j.egy.2019.11.031>.

- [36] B. Jozwiak, G. Dzido, E. Zorebski, A. Kolanowska, R. Jedrysiak, J. Dziadosz, M. Libera, S. Boncel, M. Dzida, Remarkable thermal conductivity enhancement in carbon-based ionanofluids: effect of nanoparticle morphology, *ACS Appl. Mater. Interfaces* 12 (2020) 38113–38123, https://doi.org/10.1021/ACSAMI.0C09752/ASSET/IMAGES/LARGE/AM0C09752_0006.JPEG.
- [37] A. Naddaf, S. Zeinali Heris, Experimental study on thermal conductivity and electrical conductivity of diesel oil-based nanofluids of graphene nanoplatelets and carbon nanotubes, *Int. Commun. Heat Mass Tran.* 95 (2018) 116–122, <https://doi.org/10.1016/j.icheatmasstransfer.2018.05.004>.
- [38] H. Matsubara, G. Kikugawa, T. Bessho, T. Ohara, Evaluation of thermal conductivity and its structural dependence of a single nanodiamond using molecular dynamics simulation, *Diam. Relat. Mater.* 102 (2020), 107669, <https://doi.org/10.1016/j.diamond.2019.107669>.
- [39] S. Ebrahimi, Thermal conductivity of water base Ni-np@MWCNT magnetic nanofluid, *Mater. Res. Bull.* 150 (2022), 111781, <https://doi.org/10.1016/J.MATERRESBULL.2022.111781>.
- [40] R. Hossain, A.K. Azad, M. Jahid Hasan, M.M. Rahman, Thermophysical properties of Kerosene oil-based CNT nanofluid on unsteady mixed convection with MHD and radiative heat flux, *Engineering Science and Technology, Int. J.* 35 (2022), 101095, <https://doi.org/10.1016/J.JESTCH.2022.101095>.
- [41] H. Karami, S. Papari-Zare, M. Shanbedi, H. Eshghi, A. Dashtbozorg, A. Akbari, E. Mohammadian, M. Heidari, A.Z. Sahin, C.B. Teng, The thermophysical properties and the stability of nanofluids containing carboxyl-functionalized graphene nano-platelets and multi-walled carbon nanotubes, *Int. Commun. Heat Mass Tran.* 108 (2019), 104302, <https://doi.org/10.1016/J.ICHEATMASSTRANSFER.2019.104302>.
- [42] A. Ghaffarkhah, A. Bazzi, Z. Azimi Dijvejin, M. Talebkeikhah, M. Keshavarz Moraveji, F. Agin, Experimental and numerical analysis of rheological characterization of hybrid nano-lubricants containing COOH-Functionalized MWCNTs and oxide nanoparticles, *Int. Commun. Heat Mass Tran.* 101 (2019) 103–115, <https://doi.org/10.1016/j.icheatmasstransfer.2019.01.003>.
- [43] R.K. R. M. Samykano, A.K. Pandey, K. Kadirgama, V.V. Tyagi, A comparative study on thermophysical properties of functionalized and non-functionalized Multi-Walled Carbon Nano Tubes (MWCNTs) enhanced salt hydrate phase change material, *Sol. Energy Mater. Sol. Cell.* 240 (2022), 111697, <https://doi.org/10.1016/J.SOLMAT.2022.111697>.
- [44] A. Esmaeilzadeh, N. Nik-Ghazali, H.S.C. Metselaar, M.S. Naghavi, M. Azuddin, S. Iranmanesh, Thermal performance evaluation of the heat pipe by using 1-pyrene carboxylic-acid functionalized graphene nanofluid, *Int. Commun. Heat Mass Tran.* 129 (2021), 105669, <https://doi.org/10.1016/j.icheatmasstransfer.2021.105669>.
- [45] T.O. Babarinde, S.A. Akinlabi, D.M. Madyira, Energy performance evaluation of R600a/MWCNT-nanolubricant as a drop-in replacement for R134a in household refrigerator system, *Energy Rep.* 6 (2020) 639–647, <https://doi.org/10.1016/j.egyr.2019.11.132>.
- [46] T.O. Babarinde, S.A. Akinlabi, D.M. Madyira, F.M. Ekundayo, COMPARATIVE STUDY OF ENERGY PERFORMANCE OF R600a/TiO2 AND R600a/MWCNT NANOLUBRICANTS IN A VAPOR COMPRESSION REFRIGERATION SYSTEM, *Int. J. Energy a Clean Environ. (IJECE)* 21 (2020) 317–332, <https://doi.org/10.1615/InterJenerCleanEnv.2020034660>.
- [47] A.I. Alsabery, T. Tayebi, H.T. Kadhim, M. Ghalambaz, I. Hashim, A.J. Chamkha, Impact of two-phase hybrid nanofluid approach on mixed convection inside wavy lid-driven cavity having localized solid block, *J. Adv. Res.* 30 (2021) 63–74, <https://doi.org/10.1016/j.jare.2020.09.008>.
- [48] R. Hossain, A.K. Azad, Md Jahid Hasan, M.M. Rahman, Thermophysical properties of Kerosene oil-based CNT nanofluid on unsteady mixed convection with MHD and radiative heat flux, *Eng. Sci. Tech. Int. J.* 35 (2022), 101095, <https://doi.org/10.1016/j.jestch.2022.101095>.
- [49] V. Sivalingam, P. Ganesh Kumar, R. Prabhakaran, J. Sun, R. Velraj, S.C. Kim, An automotive radiator with multi-walled carbon-based nanofluids: a study on heat transfer optimization using MCDM techniques, *Case Stud. Therm. Eng.* 29 (2022) 101724, <https://doi.org/10.1016/j.csite.2021.101724>.
- [50] A. Ghadimi, R. Saidur, H.S.C. Metselaar, A review of nanofluid stability properties and characterization in stationary conditions, *Int. J. Heat Mass Tran.* 54 (2011) 4051–4068, <https://doi.org/10.1016/J.IJHEATMASSTRANSFER.2011.04.014>.
- [51] B. White, S. Banerjee, S. O'Brien, N.J. Turro, I.P. Herman, Zeta-potential measurements of surfactant-wrapped individual single-walled carbon nanotubes, *J. Phys. Chem. C* 111 (2007) 13684–13690, <https://doi.org/10.1021/jp070853e>.
- [52] M. Lemouari, M. Boumaza, A. Kaabi, Experimental analysis of heat and mass transfer phenomena in a direct contact evaporative cooling tower, *Energy Convers. Manag.* 50 (2009) 1610–1617, <https://doi.org/10.1016/J.ENCONMAN.2009.02.002>.
- [53] P.J. Grobbelaar, H.C.R. Reuter, T.P. Bertrand, Performance characteristics of a trickle fill in cross- and counter-flow configuration in a wet-cooling tower, *Appl. Therm. Eng.* 50 (2013) 475–484, <https://doi.org/10.1016/J.APPLTHERMALENG.2012.06.026>.
- [54] J.C. Kloppers, D.G. Kröger, A critical investigation into the heat and mass transfer analysis of crossflow wet-cooling towers, <https://doi.org/10.1080/104077890504113>, 2010, 785–806.
- [55] M. Lucas, P.J. Martínez, A. Viedma, Experimental study on the thermal performance of a mechanical cooling tower with different drift eliminators, *Energy Convers. Manag.* 50 (2009) 490–497, <https://doi.org/10.1016/J.ENCONMAN.2008.11.008>.
- [56] E.M. Cardenas Contreras, E.P. Bandarra Filho, Heat transfer performance of an automotive radiator with MWCNT nanofluid cooling in a high operating temperature range, *Appl. Therm. Eng.* 207 (2022), 118149, <https://doi.org/10.1016/J.APPLTHERMALENG.2022.118149>.
- [57] A. Heidarshenas, Z. Azizi, S.M. Peyghambarzadeh, S. Sayyahi, Experimental investigation of heat transfer enhancement using ionic liquid-Al₂O₃ hybrid nanofluid in a cylindrical microchannel heat sink, *Appl. Therm. Eng.* 191 (2021), 116879, <https://doi.org/10.1016/J.APPLTHERMALENG.2021.116879>.
- [58] R.H. Chen, T.X. Phuoc, D. Martello, Effects of nanoparticles on nanofluid droplet evaporation, *Int. J. Heat Mass Tran.* 53 (2010) 3677–3682, <https://doi.org/10.1016/J.IJHEATMASSTRANSFER.2010.04.006>.
- [59] C.Y. Tso, C.Y.H. Chao, Study of enthalpy of evaporation, saturated vapor pressure and evaporation rate of aqueous nanofluids, *Int. J. Heat Mass Tran.* 84 (2015) 931–941, <https://doi.org/10.1016/J.IJHEATMASSTRANSFER.2015.01.090>.
- [60] S. Tanvir, L. Qiao, Surface tension of nanofluid-type fuels containing suspended nanomaterials, *Nanoscale Res. Lett.* 7 (2012), <https://doi.org/10.1186/1556-276X-7-226>.
- [61] O.A. Alawi, N.A.C. Sidik, The effect of temperature and particles concentration on the determination of thermo and physical properties of SWCNT-nanorefrigerant, *Int. Commun. Heat Mass Tran.* 67 (2015) 8–13, <https://doi.org/10.1016/j.icheatmasstransfer.2015.06.014>.
- [62] A. Celen, A. Çebi, M. Aktas, O. Mahian, A.S. Dalkilic, S. Wongwises, A review of nanorefrigerants: flow characteristics and applications, *Int. J. Refrig.* 44 (2014) 125–140, <https://doi.org/10.1016/j.ijrefrig.2014.05.009>.
- [63] Y.H. Diao, C.Z. Li, Y.H. Zhao, Y. Liu, S. Wang, Experimental investigation on the pool boiling characteristics and critical heat flux of Cu-R141b nanorefrigerant under atmospheric pressure, *Int. J. Heat Mass Tran.* 89 (2015) 110–115, <https://doi.org/10.1016/j.ijheatmasstransfer.2015.05.043>.
- [64] Reza Javadpour, Saeed Zeinali Heris, Yaghoob Mohammadfam, Seyed Borhan Mousavi, Optimizing the heat transfer characteristics of MWCNTs and TiO₂ water-based nanofluids through a novel designed pilot-scale setup, *Scientific Reports* 12 (1) (2022) 15154, <https://doi.org/10.1038/s41598-022-19196-3>.